Materials Science & Engineering A 700 (2017) 481–486

Contents lists available at ScienceDirect

Materials Science & Engineering A

journal homepage: www.elsevier.com/locate/msea

Effect of tungsten concentration on microstructures of Co-10Ni-6Al-(0,2,4,6) W-6Ti (at%) cobalt-based superalloys

Peter J. Bocchini[a,*], Chantal K. Sudbrack[b], Daniel J. Sauza[a], Ronald D. Noebe[b], David N. Seidman[a,c,d], David C. Dunand[a,d]

[a] Department of Materials Science and Engineering, Northwestern University, 2220 Campus Drive, Evanston, IL 60208-3108, USA
[b] NASA Glenn Research Center, 21000 Brookpark Road, Cleveland, OH 44135, USA
[c] Northwestern University Center for Atom-Probe Tomography (NUCAPT), 2220 Campus Drive, Evanston, IL 60208-3108, USA
[d] NanoAl LLC, Illinois Science + Technology Park, 8025 Lamon Ave, Suite 446, Skokie, IL 60077, USA

ARTICLE INFO

Keywords:
Cobalt alloys
Superalloy
Intermetallic
$L1_2$, grain boundary

ABSTRACT

The effects of reducing the W concentration (and concomitantly mass density) of Co-10Ni-6Al-xW-6Ti at% Co-based superalloys, with a γ(f.c.c.) plus γ′($L1_2$) microstructure, is investigated for a series of alloys with W concentrations of 6 at% (baseline alloy), 4 and 2 at% (W-reduced) and 0 at% (W-free). The γ′($L1_2$) solvus temperature decreases strongly (by 46 °C per 1 at% reduction in W), while the liquidus and solvus temperatures decrease mildly (3–5 °C per 1 at% W reduction) as measured by differential scanning calorimetry. Scanning electron microscopy was used to image phase formation in all alloys. When aging at 900 or 1000 °C for 256 h, the W reduction does not result in the appearance of additional phases within the grains beyond the γ(f.c.c.) and γ′($L1_2$) phases present in the original alloy. Grain-boundary precipitates are present for all alloy compositions: W-rich or W-free precipitates after aging at 1000 °C, and coarsened γ′($L1_2$) precipitates after aging at 900 °C. The composition of grain boundary precipitates were measured with energy-dispersive X-ray spectroscopy. Vickers microhardness values decrease with decreasing W content, due to a reduction in γ′($L1_2$) precipitation and reduced solid-solution strengthening.

1. Introduction

The study of Co-based superalloys strengthened by coherent γ′($L1_2$)-precipitates is accelerating as interest grows for their use in high-temperature structural applications, such as jet-engine turbine blades and discs and turbine blades for land-based natural gas-fired engines for generating electricity. It was long thought that the γ′($L1_2$)-precipitate phase, analogous to the primary strengthening phase in Ni-based superalloys [1–3], could not form in Co alloys [3]. Sato et al. discovered in 2006, however, that a γ(f.c.c.) plus γ′($L1_2$) two-phase microstructure forms in the Co-Al-W system [4] with a γ′($L1_2$) composition near $Co_{78}(W_{12.0–12.5}Al_{9.0–10.0})$ when aged at 900 °C [4,5]. Cobalt-superalloys have solidus and liquidus temperatures 50–150 °C higher than conventional Ni-based superalloys [4] and hence they have the potential to surpass the high-temperature capabilities of Ni-based alloys.

However, alloy mass density is a major challenge for most Co-superalloys based on the composition utilized by Sato et al. [4], because W (mass density of 19.3 g cm^{-3}) is required at high concentrations, 7–10 at% (20–27 wt%), resulting in superalloy mass densities in excess of 9.0 g cm^{-3} [6]. By comparison, the mass density of Ni-based superalloys ranges from 8.4 to 9.1 g cm^{-3}, with the highest values for alloys containing 4–6 wt% W and other high-mass density alloying additions: for example, 6–9 wt% Ta (16.4 g cm^{-3}) and 3–6 wt% Re (21.0 g cm^{-3}) [7–9]. The lowest mass densities for Ni-based superalloys are ones with 0 wt% W, with smaller Re (1.5–3.0 wt%) and Ta (6 wt%) concentrations, when 7–10 wt% Mo (10.2 g cm^{-3}) is added for additional solid-solution strengthening. Therefore, reducing the high W content of Co-superalloys is necessary to match the mass density of current Ni-based superalloys. Makineni et al. [23,24] have developed W-free Co-Ni-Al-Mo-Nb superalloys with a mass density as low as 8.4 g cm^{-3}, by replacing W with 5 at% Mo (10.2 g cm^{-3}) and 2 at% Nb (8.6 g cm^{-3}). The removal of W is accompanied, however, by a strong reduction in the γ′($L1_2$)-precipitate solvus temperature. Depending on Ni content, these alloys have solvus temperatures ranging from 866 °C for alloys containing 0 at% Ni to 990 °C for alloys with 30 at% Ni. Alternatively, Ti has been shown to be an effective substitute for W in Co-Al-W-Ti [10–12] and Co-Ni-Al-W-Ti [15] alloys, increasing the γ′($L1_2$)-solvus temperature and reducing mass density; e.g., 1137 °C and 8.8 g cm^{-3}, respectively, for a Co-10Ni-5Al-5W-8Ti at% alloy.

In order for Co-based superalloys to be adopted in the aerospace

* Corresponding author.

http://dx.doi.org/10.1016/j.msea.2017.06.018
Received 27 January 2017; Received in revised form 24 May 2017; Accepted 3 June 2017
Available online 06 June 2017

industry, they must have densities at least as low as conventional Ni-based superalloys. Tungsten (19.3 g cm^{-3}) is the highest density element in Co-based superalloys and therefore understanding the role of W in $\gamma'(L1_2)$-precipitation (and thus strength) is critical to the long-term success of these alloys. Pyczak et al. has shown that reduction of W in the ternary Co-Al-W system significantly reduces $\gamma'(L1_2)$-precipitate volume fraction where reducing W from 11 to 8 at% leads to a drop in volume fraction from 73% to 34% [14]. Furthermore, for the same decrease in W yielded a drop in $\gamma'(L1_2)$-solvus temperature from 1036 to 960 °C [14]. The present research investigates the effect of decreasing W content, up to its complete removal, in a series of Co-10Ni-6Al-xW-6Ti at% alloys (x = 6, 4, 2, 0). The intent of the present work is to build off on current understanding of W in the Co-Al-W ternary system [14,16] by investigating the higher order Co-Ni-Al-W-Ti system. Co-Al-W was alloyed with Ti [10–12] and Ni [15] because both of these additions are known to stabilize the $\gamma'(L1_2)$ two-phase microstructure. By replacing W with Ni and Ti, the overall alloy density will be reduced while maintaining strength. The microstructural stability of the $\gamma'(L1_2)$-precipitate phase is investigated employing isothermal aging treatments at 900 and 1000 °C for 256 h. Phase compositions of $\gamma'(L1_2)$-precipitates and grain boundary (GB) precipitates are measured utilizing energy-dispersive X-ray spectroscopy (EDS). Room temperature Vickers microhardness measurements are utilized to compare mechanical properties. This work aims to further the understanding of low W Co-based superalloys and the role of W on the precipitation kinetics of the $\gamma'(L1_2)$ phase.

2. Experimental methods

Button ingots of ~ 50 g were produced with nominal compositions of Co-10Ni-6Al-xW-6Ti at% (x = 6, 4, 2, 0), which correspond to Co-10Ni-3Al-xW-5Ti wt% (x = 19, 13, 6, 0). The alloys are herein denoted as 6W, 4W, 2W and 0W, respectively, with their concentrations given in at%. The alloys were produced using high purity Co (99.9%), Al (99.999%), Ni (99.995%), Ti (99.995%) and a Co-10Ni-9Al-9W cast master alloy arc-melted under a partial Ar atmosphere; the ingots were flipped four times between each melting step to guarantee a homogenous distribution of the constituent elements. Bulk compositions were measured using inductively-coupled plasma atomic-emission spectroscopy (ICP-AES) using ~ 1 g samples (Table 1).

The 0W, 2W and 4W alloys were homogenized in a high-vacuum furnace at 1200 °C for 24 h followed by furnace cooling. Due to a higher W content, the 6W alloy was homogenized at a higher temperature, 1240 °C for 24 h, and then furnace-cooled. The samples utilized to investigate the high-temperature stability of the $\gamma'(L1_2)$-precipitates were wrapped in a Ta foil and encapsulated in quartz tubes, which were flushed with Ar and evacuated, then aged at 900 °C or 1000 °C for 256 h, and quenched into ice water. The 900 °C and 1000 °C aging temperatures were chosen to match Pyczak et al.'s study on the effect of W in a ternary Co-Al-W alloy [14]. Similarly, the 256 h aging time was chosen to be comparable to the 200 h used by Pyczak et al. and is sufficiently long to observe the precipitation and potential decomposition of the $\gamma'(L1_2)$-phase.

Vickers microhardness measurements were performed at ambient temperature utilizing a Struers Duramin-5 microhardness tester, with an applied load of 1 kg and a dwell time of 5 s. Measurements were made across multiple grains on samples that were polished to a 1 μm finish.

Scanning electron microscopy (SEM) images and energy-dispersive X-ray spectroscopy (EDS) composition measurements were recorded using a Hitachi S-3400N-II SEM equipped with an Oxford INCAx-act SDD EDS detector. The samples used for SEM imaging were polished to a 1 μm finish and imaged in an unetched condition. The volume fraction, ϕ, for $\gamma'(L1_2)$-precipitates was measured by the line-intercept method [17] on SEM images recorded near a {100}-type plane. Differential scanning calorimetry (DSC) experiments were performed under He to measure the $\gamma'(L1_2)$-solvus temperatures of the 0W, 2W, and 4W alloys aged at 900 °C for 16 h. Single cycle experiments at a heating rate of 5 °C min^{-1} were used to identify the $\gamma'(L1_2)$-solvus, solidus, and liquidus temperatures during heating. All data for the 6W alloy, with the exception of the 900 °C micrographs and microhardness measurements, were taken from our prior work [13].

Table 1
Bulk compositions of Co-10Ni-6Al-xW-6Ti at% alloys as measured by ICP-AES. Data for Co-10Ni-6Al-6W-6Ti is taken from Ref. [13].

Alloy	Concentration (at%)				
	Co	Ni	Al	W	Ti
10Ni-6Al-0W-6Ti	78.1	10.0	5.8	–	6.2
10Ni-6Al-2W-6Ti	75.9	10.0	5.9	2.0	6.1
10Ni-6Al-4W-6Ti	73.9	10.1	5.7	3.9	6.2
10Ni-6Al-6W-6Ti	71.6	10.1	5.2	6.7	6.4

3. Results and discussion

3.1. Microstructure

After 256 h of aging at 900 °C (Fig. 1), the 2W, 4W and 6W alloys form a γ(f.c.c.) plus $\gamma'(L1_2)$ microstructure, while only a single-phase γ(f.c.c.) microstructure is present in the W-free (0W) alloy. The 4W and 6W alloys contain large volume fractions (58 ± 5 and 73 ± 2%, respectively) of highly-aligned cuboidal $\gamma'(L1_2)$-precipitates most of which, in the 6W alloy, are coalesced and form lath-shaped structures. The 2W alloy aged at 900 °C contains aligned $\gamma'(L1_2)$-precipitates, but at a much smaller volume fraction (19 ± 2%) than the 4W and 6W alloys, which have coarsened in the < 100 > -type direction to form elongated precipitates. The morphological evolution of the $\gamma'(L1_2)$-precipitates at 900 °C in the 4W and 6W alloys is comparable from what has been observed in the Co-Al-W system [14] where the $\gamma'(L1_2)$-precipitates retain their cuboidal shape. The elongated round $\gamma'(L1_2)$-precipitates observed in the 2W alloy is more comparable to Co-Al-W-Ti alloys aged at 1000 °C for 1000 h [11]. The volume fraction of the Co-Ni-Al-W-Ti samples drops 13.5% per one at% W, which matches almost exactly the 13% per one at% W measured in the Co-Al-W system by Pyczak et al. [14] (aged at 900 °C) and 14% per one at% W measured by Ooshima et al. [16] (aged at 850 °C).

After 256 h of aging at 1000 °C, only the 4W and 6W alloys exhibit a γ(f.c.c.) plus $\gamma'(L1_2)$ microstructure, while the 0 W and 2W alloys consist of only a single–phase γ(f.c.c.). The 4W and 6W alloys aged at 1000 °C have smaller $\gamma'(L1_2)$ volume fractions than when aged at 900 °C: 27 ± 4 and 37 ± 2% compared to 58 ± 5 and 73 ± 2%, respectively (Table 2). The $\gamma'(L1_2)$ precipitates are larger in the alloys aged at 1000 °C than at 900 °C, indicative of coarsening, (Ostwald Ripening) and are rounded rather than cuboidal. The precipitates in both the 4W and 6W alloys are highly coalesced, forming large precipitates formed from multiple smaller precipitates. Small volume fractions of the Co-24W-5Ni-1Al-13Ti phase, with a needle-like morphology (which typically correspond to the $D0_{19}$-Co_3W phase) were found in the grain interior of the 4W (~3 vol%) and 6W (~1–2 vol%) alloys aged at 1000 °C, which are visible in Fig. 2. No phases other than the γ(f.c.c.), with and without $\gamma'(L1_2)$-precipitates, were observed at grain interiors for the remainder of the alloys and aging conditions. The morphological evolution of the $\gamma'(L1_2)$-precipitates at 1000 °C in the 4W and 6W alloys is comparable to Co-Al-W-Ti alloys aged at 1000 °C for 1000 h [11]. The volume fraction of the Co-Ni-Al-W-Ti samples drops only 5% per 1 at% W which is lower than the samples aged at 900 °C as well as the 13% and 14% per 1 at% W measured in the Co-Al-W system aged at 900 °C [14] and 850 °C [16].

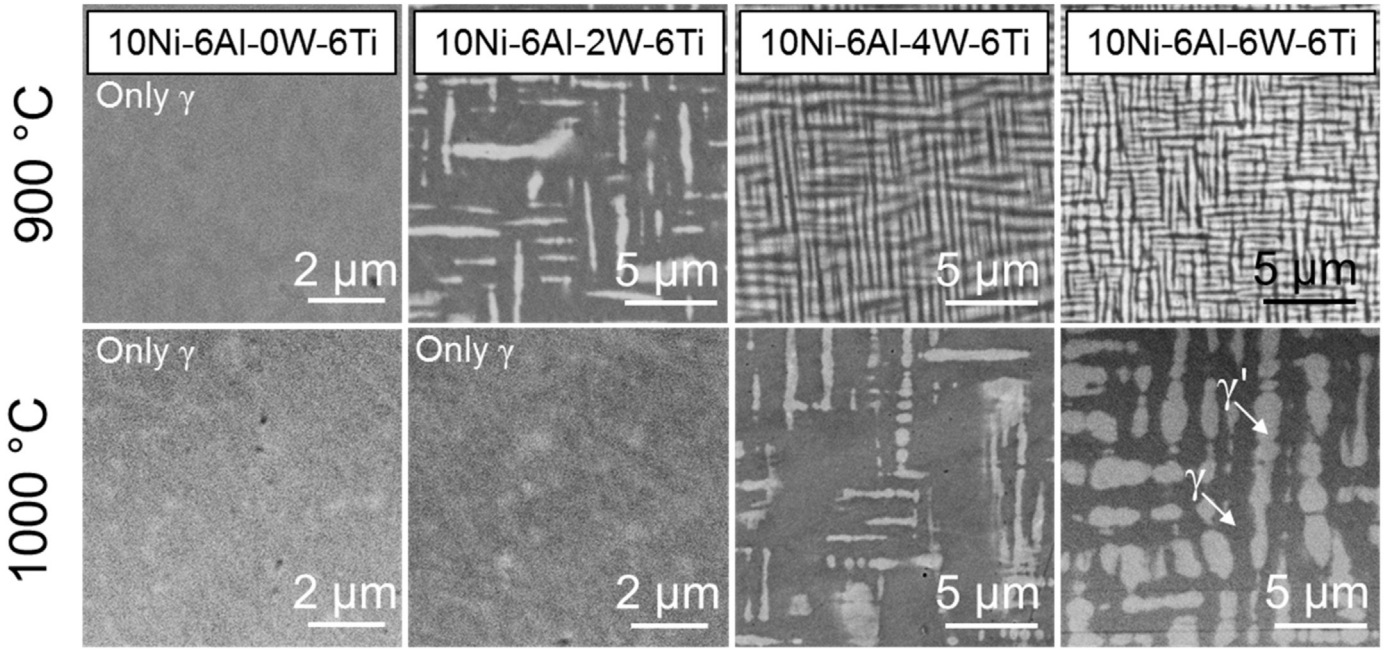

Fig. 1. Backscattered scanning electron micrographs of the γ(f.c.c.) plus γ′($L1_2$) microstructure in all alloys aged at 1000 °C for 256 h.

3.2. Grain boundary phases

The GB morphology of the 2W, 4W, and 6W alloys consist of coarsened γ′($L1_2$)-precipitates after aging at 900 °C for 256 h (Fig. 2). The 0W alloy does not contain γ′($L1_2$)-precipitates (or any other phases) in the grain interior or at the GB. After 256 h of aging at 1000 °C, all alloys' GBs develop micron-sized precipitates. The GB precipitates in the 0W alloy have a composition of Co-8Ni-1Al-13Ti at%, and are probably Co_3Ti-type ($L1_2$) precipitates [18], located within 0.5 mm of the sample's surface (Fig. 3), which may indicate that these precipitates form due to the evaporation of Al from the specimen's surface during aging. The 2 W alloy contains a small amount of a similar W-free GB precipitate phase (Co-8Ni-1Al-12Ti at%, with widths of 18–30 μm, not displayed) as well as W-rich Co-5Ni-1Al-11W-21Ti GB precipitates (Fig. 2); many of the GBs are, however, also precipitate-free. The 4W and 6W alloys also contain W-rich GB precipitates, which cover nearly the entire grain boundary area.

The compositions of the W-rich GB precipitates in the 2W, 4W, and 6W alloys vary with bulk alloy's composition (Fig. 4). The concentration of Ti in the precipitate phase decreases from 21 at% in the 2W alloy to 12 at% in the 6W alloy. Conversely, the W concentration increases from 11 at% in the 2W alloy to 33 at% in the 6W alloy, indicating that Ti is partially substituting for W in the GB precipitates with decreasing bulk W concentration. The atomic ratio Co:(W plus Ti) is 2:1 in the 2W and 4W alloys and 7:6 in the 6W alloy. The GB-precipitates in the 2W and 4W alloys may therefore be a Co_3W-type phase ($D0_{19}$)[19] or possibly a Co_3Ti-type ($L1_2$)-phase [18]. The needle-like morphology of the precipitates and the high W-content make $D0_{19}$ more likely [20]. The W concentration of the GB precipitate phase more than doubles from 14 at % in the 4W alloy to 33 at% in the 6W alloy. The 7:6 ratio of Co to W plus Ti indicates a possible transition from $D0_{19}$ to $Co_7(W,Ti)_6$ μ-type structure [4,19,21]. Similar GB μ-type phases have been observed in other Co-Ni-Al-W-Ti alloys [13]. The GB precipitates do not extend significantly into the grains and do not destabilize the γ(f.c.c.) plus γ′($L1_2$) microstructure after 256 h of aging. The effect of these GB precipitates on the mechanical properties and microstructure during loading is unknown and requires further research.

3.3. γ′($L1_2$)-Solvus, solidus, and liquidus temperatures

The γ′($L1_2$)-solvus temperature as well as the solidus and liquidus temperatures as a function of W content are summarized in Fig. 5. The concentration of W in the bulk alloy has a significant influence on the γ′($L1_2$)-solvus temperature; for a decrease of 1 at% W, the solvus temperature decreases by 46 °C. This solvus decrease is higher than 25 °C [14] and 18.5 °C [16] per 1 at% W previously observed in the Co-Al-W system. The γ′($L1_2$)-solvus in the 0W alloy was not observed utilizing DSC analyses. The samples used in the DSC measurements were aged at 900 °C, where no γ′($L1_2$)-precipitates were observed in the 0W alloy (Fig. 1). Since no γ′($L1_2$)-precipitates were present in the sample, the DSC analysis was not able to measure the solvus temperature. The Co-Ti binary phase diagram suggests that $L1_2$-Co3Ti should form at a temperature below ~800 °C; the solvus temperature is between 770 and 820 °C for the Ti concentration present in the 0W alloy [18]. The

Table 2
Volume fraction, ϕ, Vickers microhardness, and mass density of the Co-10Ni-6Al-xW-6Ti alloys after aging at 900 °C and 1000 °C for 256 h.

Alloy	Aging temperature for 256 h (°C)	ϕ (%)	Vickers microhardness (GPa)	Mass density (g cm^{-3})
10Ni-6Al-0W-6Ti	900	–	1.80 ± 0.07	8.20 ± 0.01
	1000	–	2.16 ± 0.07	
10Ni-6Al-2W-6Ti	900	19 ± 2	2.25 ± 0.03	8.54 ± 0.01
	1000	–	2.60 ± 0.05	
10Ni-6Al-4W-6Ti	900	58 ± 5	2.83 ± 0.07	8.86 ± 0.04
	1000	27 ± 4	2.67 ± 0.06	
10Ni-6Al-6W-6Ti	900	73 ± 3	3.02 ± 0.05	9.17 ± 0.02
	1000	37 ± 2	2.86 ± 0.05	

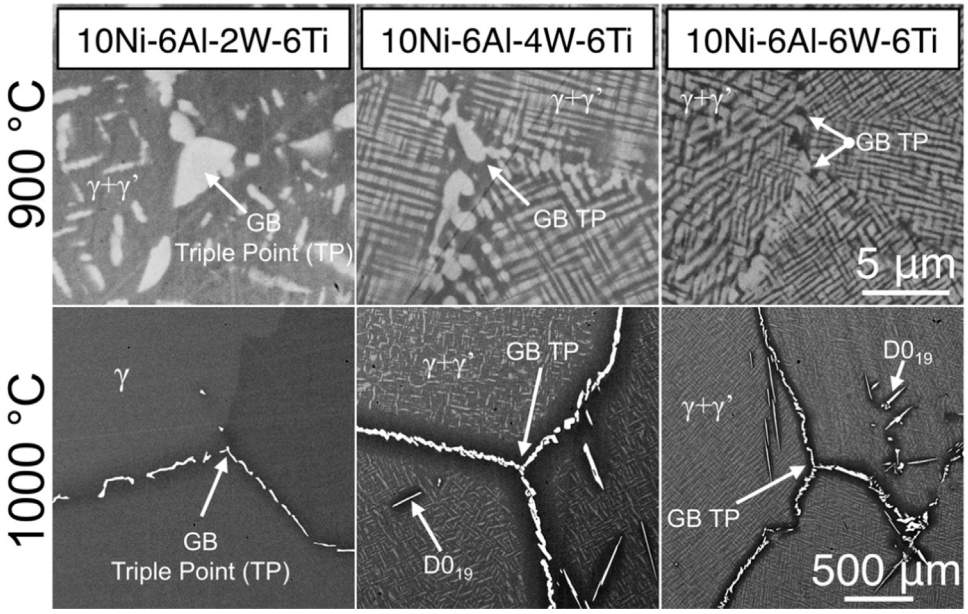

Fig. 2. Backscattered scanning electron micrographs of grain boundaries meeting at triple points in 2W, 4W, 6W alloys after 256 h of aging at 900 and 1000 °C.

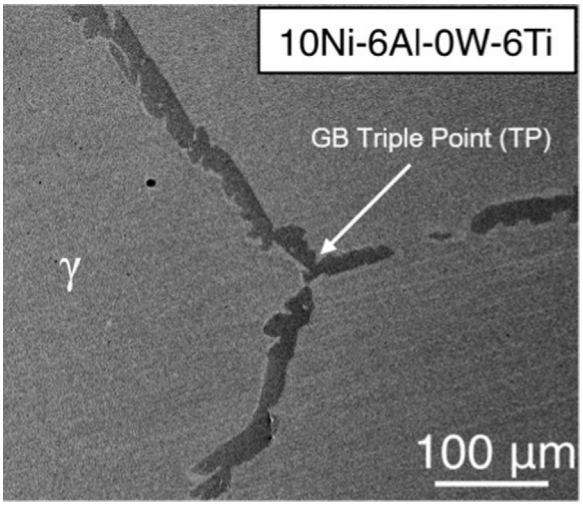

Fig. 3. Backscattered scanning electron micrographs of a grain boundary triple point in the 0W alloy after 256 h of aging at 1000 °C. GB precipitates are shown in darker contrast while the γ(f.c.c.)-matrix is shown in lighter contrast.

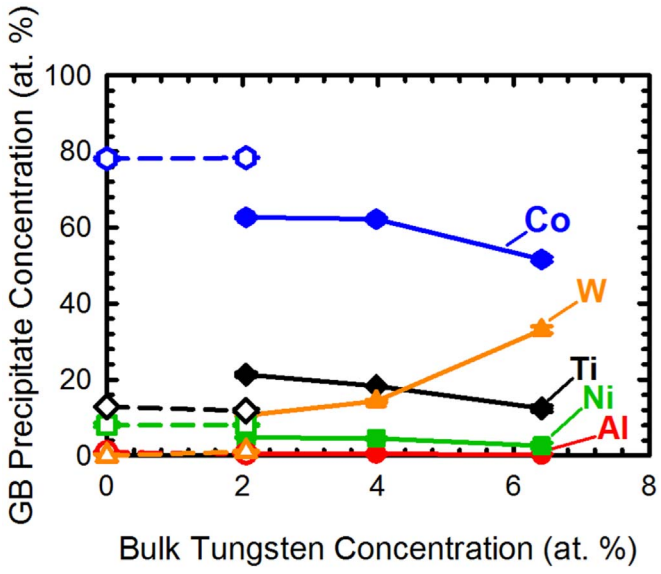

Fig. 4. Energy dispersive spectroscopy (EDS) composition of W-rich (closed symbols) and W-free (open symbols) grain boundary (GB) precipitates in all alloys aged for 256 h at 1000 °C. Data for Co-10Ni-6Al-6W-6Ti is taken from [13].

extrapolated γ′($L1_2$)-solvus temperature for the 0W alloy is 845 °C, which is slightly higher than anticipated from the Co-Ti binary phase diagram because of the additional alloying elements, Ni and Al. Solidus and liquidus temperatures are less affected by a reduced W content than the γ′($L1_2$)-solvus temperature. For a 1 at% reduction in the bulk W concentration, the solidus and liquidus temperatures decrease by 3 and 5 °C, respectively.

For comparison, the solvus temperatures are in the range of 1260–1330 °C [22] for current Ni-superalloys and 866–990 °C for W-free Co-superalloys with varying Ni concentrations [23]. Additionally, the solidus temperature for the ternary Co-9.2Al-9.0W at% alloy, originally investigated by Sato et al., is ~1450 °C, which is 130–150 °C higher than the values for the 0W–6W alloys and 50–150 °C higher than typical Ni-superalloys [4]. Reducing the W concentration decreases the mass density and the addition of Ti increases the γ′($L1_2$)-solvus temperature, with the tradeoff being lower solidus and liquidus temperatures. Additional alloying with the relatively low mass density refractory elements, such as Mo (10.28 g cm^{-3}), may offset some of the melting temperature penalty, while maintaining a weight savings from the W reduction [7,23,24].

3.4. Mass density

Reducing the W concentration substantially decreases the mass density of Co-10Ni-6Al-xW-6Ti at% alloys: for each 1 at% W decrease, the alloy's mass density decreases by 2% or 0.15 g cm^{-3} (Fig. 6). The 0 W alloy has a low mass density of 8.2 g cm^{-3} but it does not contain the desired γ(f.c.c.) plus γ′($L1_2$) microstructure at 900 or 1000 °C, thereby limiting strongly its usefulness as a structural high-temperature alloy. The 2W alloy has a mass density of 8.5 g cm^{-3} and it contains 0.19% volume fraction of γ′($L1_2$)-precipitates at 900 °C, but zero at 1000 °C because of its low solvus temperature (923 °C). The 4W and 6W alloys contain large γ′($L1_2$) volume fractions (0.58 and 0.73) at 900 °C. And still contain 0.27–0.37 vol fraction of γ′($L1_2$) at 1000 °C, given their higher solvus temperatures, with mass densities of 8.9 and 9.2 g cm^{-3} for 4W and 6W alloys, respectively. The 4W alloy is within the mass density range (8.4–9.1 g cm^{-3}) of conventional mass density-reduced Ni-based superalloys [7–9], while the 6W alloy is slightly above this range.

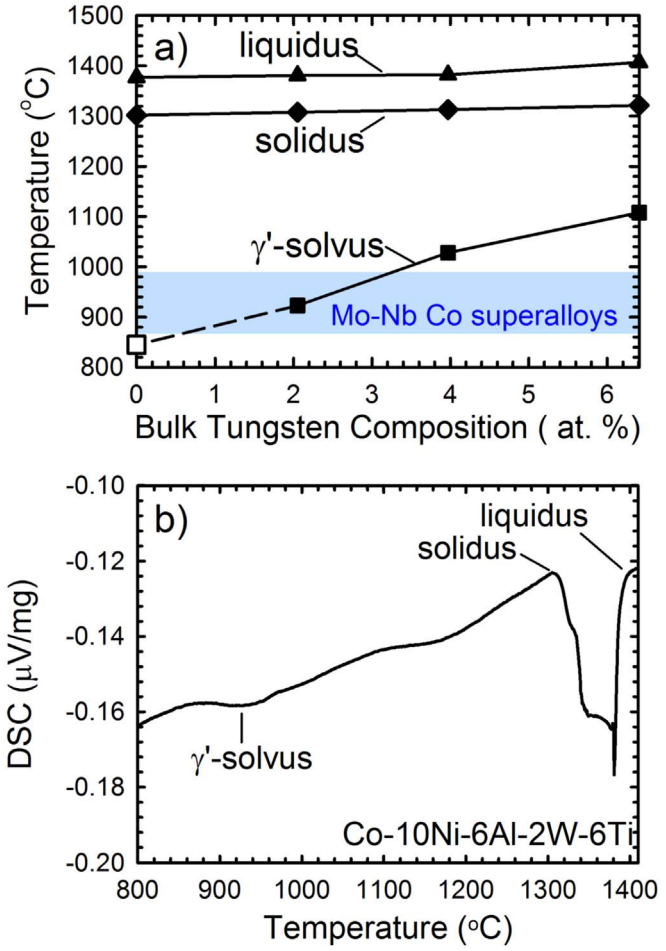

Fig. 5. a) $\gamma'(L1_2)$-solvus, solidus, and liquidus temperatures in all alloys as a function of bulk W concentration. The range of $\gamma'(L1_2)$-solvus temperatures for W-free Co-Ni-Al-Mo-Nb alloys is presented in blue [23,24]. Data for Co-10Ni-6Al-6W-6Ti is taken from [13]. b) DSC curve of the Co-10Ni-6Al-2W-6Ti alloy.

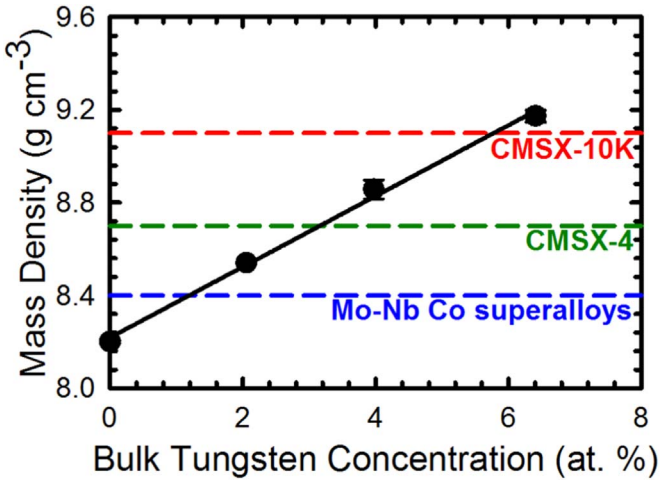

Fig. 6. Mass density in all alloys compared with Ni- and Co-based superalloy data from the literature [9,23,24]. Data for Co-10Ni-6Al-6W-6Ti is taken from [13].

3.5. Microhardness

The room temperature Vickers microhardness values increase near linearly with increasing W concentration of the bulk alloy (Fig. 7). After 256 h of aging at 900 °C, the Vickers microhardness increases from 1.8 ± 0.2 GPa in the 0W alloy to 3.0 ± 0.1 GPa in the 6W alloy. A similar increase in strength is realized after 256 h of aging at 1000 °C, where the microhardness increases from 2.2 ± 0.1–2.9 ± 0.1 GPa from increasing the bulk W concentration from 0 to 6W. The microhardness increase is probably due primarily to an increased volume fraction of $\gamma'(L1_2)$-precipitates, though increased solid-solution strengthening or atomic clusters due to W in the γ(f.c.c.)-matrix cannot be ruled out. The microhardness of the 0W alloy aged at 1000 °C is 0.4 GPa higher than the same alloy aged at 900 °C, which may indicate that small $\gamma'(L1_2)$-precipitates or even atom clusters, which are not visible utilizing SEM, formed during quenching. Similarly, the difference in microhardness between the 2W alloy aged at 900 °C and 1000 °C, 2.25 vs 2.6 GPa, respectively, may also be attributed to small $\gamma'(L1_2)$-precipitates in the latter, which are not visible by SEM, versus the larger precipitates formed at 900 °C. The microhardness values of the 4W and 6W alloys aged at 1000 °C are 6% smaller than for the same alloys aged at 900 °C because of a smaller volume fraction of $\gamma'(L1_2)$-precipitates. The microhardness of a ternary Co-9.5Al-7.5W (at%) alloy aged at 900 °C for 16 h has been measured to be 2.9 GPa [25] which is comparable to the 4W and 6W alloys aged at 900 °C in this study and higher than the 0W and 2W alloys aged at 900 °C.

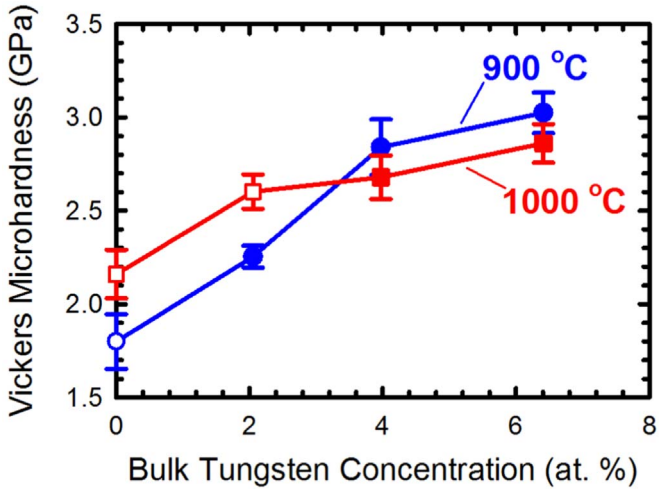

Fig. 7. Room temperature Vickers microhardness data of all alloys after 256 h of aging at 900 and 1000 °C. Hollow symbols are for alloys where $\gamma'(L1_2)$ precipitates were not observed by SEM, though finer precipitates may be present. Data for Co-10Ni-6Al-6W-6Ti aged at 1000 °C is taken from [13].

Overall, while decreasing the bulk W content reduces alloy mass density, a concomitant decrease in the $\gamma'(L1_2)$ volume fraction, due to a decreased solvus temperature, and a concomitant decrease in strength is problematic for high-temperature alloy design. The present research has focused on using Ti as a partial replacement for W to increase $\gamma'(L1_2)$ stability. An alternative approach would be to use Ta and Nb, which are known to be potent solvus temperature raisers [26–28], although the advantages in mass density reduction would not be as significant. Additionally, $\gamma'(L1_2)$-strengthened Co-Ni-Al-Mo-Nb alloys containing 5 at% Mo and 2 at% Nb, with densities of 8.4 g cm^{-3}, have been developed to replace W containing alloys entirely [23,24]. Future development of Co-based superalloys will most likely focus on some combination of Ti, Ta, Nb, and Mo additions to achieve higher solvus temperatures, while maintaining mass densities competitive with Ni-based superalloys. Additionally, Co-based superalloys display a positive γ(fcc)/$\gamma'(L1_2)$ lattice parameter mismatch (the exact value is dependent on composition), which has been suggested to improve creep strength [29] due to rafting of $\gamma'(L1_2)$-precipitates parallel to the tensile direction during mechanical loading, which is opposite to the behavior of Ni-based superalloys [30] and may ultimately provide a distinct advantage for these new Co-based alloys in certain applications.

4. Summary

A series of Co-10Ni-6Al-xW-6Ti (x = 6, 4, 2, 0) at% alloys were cast and aged at 900 and 1000 °C for 256 h to obtain a γ(f.c.c.)-matrix plus γ′($L1_2$)-precipitates microstructure. The effect of reducing the W concentration on the aged microstructure (γ′($L1_2$) stability and GB phases) and the resulting microhardness were investigated. The following conclusions are reached.

- All alloys in the Co-10Ni-6Al-xW-6Ti series, when aged below their solvus, form a γ(f.c.c.) plus γ′($L1_2$) microstructure, without any additional phase(s) being present within the bulk grains.
- Grain-boundary precipitates with W-free (found in 0W and 2W alloys) and W-rich (found in 2W, 4W and 6W alloys) compositions form upon aging at 1000 °C, whereas only coarsened γ′($L1_2$)-precipitates are present at grain boundaries after aging at 900 °C.
- For each 1 at% reduction in W content the γ′($L1_2$)-solvus temperature decreases by 46 °C, with an order of magnitude smaller effect on the liquidus and solidus temperatures.
- For each 1 at% reduction in W content the mass density of the Co-based superalloys decreases by 0.15 g cm^{-3} or 2%.
- Reducing the W-concentration decreases the microhardness values, due to reductions in precipitation strengthening (due to a smaller γ′($L1_2$) volume fractions) and solid-solution strengthening caused by a decrease in the W concentration of the alloys.

Acknowledgements

This research was supported by the US Department of Energy, Office of Basic Energy Sciences (Dr. John Vetrano, grant monitor) through grant DE-FG02-98ER45721. PJB received partial support from the NASA Aeronautics Scholarship Program (Grant No. NNX14AF45H) and Fixed Wing project. This research made use of the Optical Microscopy and Metallography (OMM) Facility, which receives support from the Materials Research Science and Engineering Center (MRSEC) Program (DMR-112162) at Northwestern University. This research also made use of the Electron Probe Instrumentation Center (EPIC) facility of the Northwestern University Atomic and Nanoscale Characterization Experimental Center (NUANCE), which receives support from the Materials Research Science and Engineering Center (MRSEC) program (NSF DMR-1121262); the International Institute for Nanotechnology (IIN); and the State of Illinois, through the IIN. The authors also thank Messrs. Jesse Bierer and Grant Feichter (NASA Glenn Research Center, Cleveland, OH) for their assistance with arc-melting and heat-treating the specimens.

References

[1] M. Durand-Charre, The Microstructure of Superalloys, Gordon and Breach Science Publishers, Amsterdam, 1997.
[2] R.C. Reed, The Superalloys, Cambridge University Press, New York, 2006.
[3] C.T. Sims, N.S. Stoloff, W.C. Hagel, Superalloys II, John Wiley & Sons Inc., New York, 1987.
[4] J. Sato, T. Omori, K. Oikawa, I. Ohnuma, R. Kainuma, K. Ishida, Cobalt-base high-temperature alloys, Science 312 (2006) 90–91.
[5] P.J. Bocchini, E.A. Lass, K. Moon, M.E. Williams, C.E. Campbell, U.R. Kattner, D.C. Dunand, D.N. Seidman, Atom-probe tomographic study of γ/γ' interfaces and compositions in an aged Co-Al-W superalloy, Scr. Mater. 68 (2012) 563–566.
[6] H.-Y. Yan, V.A. Vorontsov, D. Dye, Alloying effects in polycrystalline γ′ strengthened Co–Al–W base alloys, Intermetallics 48 (2014) 44–53.
[7] R.A. MacKay, T.P. Gabb, J.L. Smialek, M.V. Nathal, A new approach of designing superalloys for low density, JOM 62 (2010) 48–54.
[8] T.M. Pollock, S. Tin, Nickel-based superalloys for advanced turbine engines: chemistry, microstructure, and properties, JPP 22 (2006) 361–374.
[9] W.S. Walston, K.S. O'Hara, E.W. Ross, T.M. Pollock, W.H. Murphy, Rene N6: third generation single crystal superalloy, Superalloys (1996) 27–34.
[10] C.H. Zenk, S. Neumeier, H.J. Stone, M. Göken, Mechanical properties and lattice misfit of γ/γ′ strengthened Co-base superalloys in the Co–W–Al–Ti quaternary system, Intermetallics 55 (2014) 28–39.
[11] S. Kobayashi, Y. Tsukamoto, T. Takasugi, Phase equilibria in the Co-rich Co-Al-W-Ti quaternary system, Intermetallics 19 (2011) 1908–1912.
[12] F. Xue, H.J. Zhou, X.F. Ding, M.L. Wang, Q. Feng, Improved high temperature γ′ stability of Co–Al–W-base alloys containing Ti and Ta, Mater. Lett. 112 (2013) 215–218.
[13] P.J. Bocchini, C.K. Sudbrack, D.J. Sauza, R.D. Noebe, D.N. Seidman, Effect of Ti Substitution of Al and W in Co-10Ni-9Al-9W (at%) Superalloys, (submitted for publication).
[14] F. Pyczak, A. Bauer, M. Göken, U. Lorenz, S. Neumeier, M. Oehring, J. Paul, N. Schell, A. Schreyer, A. Stark, F. Symanzik, The effect of tungsten content on the properties of L12-hardened Co–Al–W alloys, J. Alloy. Compd. 632 (2015) 110–115.
[15] K. Shinagawa, T. Omori, J. Sato, K. Oikawa, I. Ohnuma, R. Kainuma, K. Ishida, Phase equilibria and microsctructure on γ′ phase in Co-Ni-Al-W system, Mater. Trans. JIM 49 (2008) 1474–1479.
[16] M. Ooshima, K. Tanaka, N.L. Okamoto, K. Kishida, H. Inui, Effects of quaternary alloying elements on the γ′ solvus temperature of Co–Al–W based alloys with fcc/L12 two-phase microstructures, J. Alloy. Compd. 508 (2010) 71–78.
[17] J.C. Russ, R.T. Dehoff, Practical Stereology, 2nd ed., Springer, New York, New York, 1986.
[18] J.L. Murray, Co-Ti (Cobalt-Titanium), Binary Alloy Phase Diagrams, 2nd ed., ASM International, Materials Park, 1990.
[19] A. Markström, K. Frisk, B. Sundman, A revised thermodynamic description of the Co-W-C system, J. Phase Equilibria Diffus. 26 (2005) 152–160.
[20] D.J. Sauza, P.J. Bocchini, D.C. Dunand, D.N. Seidman, Influence of ruthenium on microstructural evolution in a model CoAlW superalloy, Acta Mater. 117 (2016) 135–145.
[21] F. Xue, M. Wang, Q. Feng, Alloying effects on heat-treated microstructure in Co-Al-W base superalloys at 1300 °C and 900 °C, Superalloys 12 (2012) 813–821.
[22] P. Caron, High γ' solvus new generation nickel-based superalloys for single crystal turbine blade applications, Superalloys (2000) 737–746.
[23] S.K. Makineni, B. Nithin, K. Chattopadhyay, Synthesis of a new tungsten-free γ–γ′ cobalt-based superalloy by tuning alloying additions, Acta Mater. 85 (2015) 85–94.
[24] S.K. Makineni, B. Nithin, K. Chattopadhyay, A new tungsten-free γ–γ' Co–Al–Mo–Nb-based superalloy, Scr. Mater. 98 (2015) 36–39.
[25] P.J. Bocchini, C.K. Sudbrack, R.D. Noebe, D.C. Dunand, D.N. Seidman, Microstructural and creep properties of boron- and zirconium-containing cobalt-based superalloys, Mater. Sci. Eng.: A 682 (2017) 260–269.
[26] T. Omori, K. Oikawa, J. Sato, I. Ohnuma, U.R. Kattner, R. Kainuma, K. Ishida, Partition behavior of alloying elements and phase transformation temperatures in Co-Al-W-base quaternary systems, Intermetallics 32 (2013) 274–283.
[27] A. Bauer, S. Neumeier, F. Pyczak, M. Göken, Creep strength and microstructure of polycrystalline γ′ – strengthened cobalt-base superalloys, Superalloys 12 (2012) 695–703.
[28] A. Bauer, S. Neumeier, F. Pyczak, R.F. Singer, M. Göken, Creep properties of different γ′-strengthened co-base superalloys, Mater. Sci. Eng. A 550 (2012) 333–341.
[29] H. Mughrabi, The importance of sign and magnitude of γ/γ′ lattice misfit in superalloys—with special reference to the new γ′-hardened cobalt-base superalloys, Acta Mater. 81 (2014) 21–29.
[30] Q. Liu, J. Coakley, D.N. Seidman, D.C. Dunand, Precipitate evolution and creep behavior of a W-free co-based superalloy, Metall. Mater. Trans. A 47 (2016) 6090–6096.